文章编号: 1001－2060(2008)04－0425－04

水煤浆流经小曲率半径弯管的阻力特性研究

刘　猛, 陈良勇, 段钰锋
(东南大学 能源与环境学院, 江苏 南京 210096)

摘　要: 在自制试验台上研究了水煤浆流经小曲率半径 90° 水平弯管的局部阻力特性, 分析了不同的曲率半径 R_c 对弯管的局部压力损失、压力损失系数以及摩擦阻力损失之比的影响。结果表明: 随着雷诺数 Re 的增加, 弯管的局部压力损失增大, 而压力损失系数先降低后增加。考虑到曲率半径较小, 弯管的局部压力损失由不规则流动损失与弯管轴线加长所产生的沿程阻力决定。弯管曲率半径越大, 临界雷诺数就越大。弯管摩擦阻力损失之比随着 Dean 数的增加先降后升。R_c/R 为 4.0 的弯管的局部压力损失、压力损失系数以及摩擦阻力损失之比均最小。

关　键　词: 水煤浆; 曲率半径; 压力损失系数; 临界雷诺数
中图分类号: O373　　文献标识码: A

引　言

水煤浆是一种液固两相的非牛顿流体, 也是一种很有发展潜力的新型燃料。从长远来看, 水煤浆要被大量用于工业生产, 其中必然会涉及到水煤浆的输送问题。目前国内水煤浆的技术研究主要集中在制浆、雾化燃烧、流变特性、触变性和稳定性等方面, 但在管道输送方面尚有许多问题需要解决, 如管道泵的特性、管道阻力的预测、管道局部装置流动阻力的计算等等, 特别对局部装置中的流动研究甚少, 而国外学者对非牛顿流体流经局部装置的阻力特性做了很多研究, Turian 引用局部阻力系数得出了非牛顿流体流经突扩、突缩、弯管等局部管件的阻力压降[1]。S. Gh. Etema 引用了无量纲的阻力系数[2], 研究了湍流状态下的非牛顿流体流经各种局部管件(突扩、突缩、球阀、90° 弯管和门阀等)的阻力特性, 并且得出了计算各种局部管件阻力系数的经验公式。Tarun 同样也获得了计算非牛顿流体流经各种小直径局部管件压力损失的经验式[3]。

目前对非牛顿流体流经弯管的局部阻力特性的研究主要集中在具有较大曲率半径 R_c($R_c/R>10$, 其中 R 为圆管半径)的水平弯管上, Nigam 列举了许多工程上用于研究较大曲率半径弯管阻力特性的经验式[4]。Singh 等人采用经验式计算了非牛顿流体流经较大曲率半径弯管的轴线压力梯度[5]。但只有少数人对非牛顿流体流经小曲率半径($R_c/R<10$)的 90° 水平弯管的局部阻力特性进行过研究, Mukhtar 采用压降比 $\Delta P_b/\Delta P_{st}$(ΔP_b 为弯管段的压降, ΔP_{st} 为与弯管轴线长度相等的沿程直管段上的压力损失)与流量的关系研究了多种非牛顿流体流经弯管($R_c/R=4$)的局部阻力特性[6]。Marn 研究了灰水混合物(剪切变稠)流经弯管($R_c/R=2$)的局部阻力特性[7]。但是他们都没有考虑到曲率半径的变化对弯管局部阻力特性的影响, 而本文主要研究了高粘度的水煤浆流经具有小曲率半径的 90° 水平弯管时, 曲率半径的变化对弯管局部阻力特性的影响。

1　理论方法

目前, 对于水平弯管局部压力损失有两种定义: 一种是对弯管自身几何长度内的压力损失而言; 另一种是对弯管所影响管段内的全部损失(局部加沿程损失)而言。本研究对弯管的局部压力损失采用第二种定义。

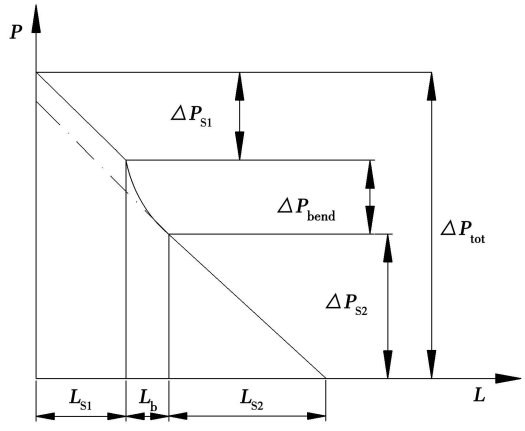

图 1　弯管的压力分布

收稿日期: 2007－08－02;　修订日期: 2007－08－30
基金项目: 国家重点基础研究发展计划(973)基金资助项目(2004CB217701)
作者简介: 刘　猛(1983－), 男, 江苏盐城人, 东南大学硕士研究生.

如图 1 所示，弯管的压力损失主要是由两个部分组成：一部分是弯管的局部压力损失 ΔP_{bend}，另一部分是弯管段前后直管段的压力损失 ΔP_s，则弯管的总压力损失 ΔP_{tot} 表示为：

$$\Delta P_{tot} = \Delta P_{bend} + \Delta P_s \tag{1}$$

弯管段前后直管段的压降采用下式来计算：

$$\Delta P_s = \Delta P_{s1} + \Delta P_{s2} = \frac{(L_{s1}+L_{s2})}{D} \cdot \lambda \cdot \frac{\rho v^2}{2} \tag{2}$$

式中：L_{s1}、L_{s2}—弯管前后直管段的长度；v—管内的平均流速；ρ、D—水煤浆密度和圆管直径，对于阻力系数 λ 我们采用 Darey-Weisbach 摩擦阻力系数：

$$\lambda = 64/Re \tag{3}$$

因此弯管的局部压力损失 ΔP_{bend} 为：

$$\Delta P_{bend} = \Delta P_{tot} - \Delta P_s = \Delta P_{tot} - \frac{(L_{s1}+L_{s2})}{D} \cdot \lambda \cdot \frac{\rho v^2}{2} \tag{4}$$

Oliveira 等人用压力损失系数研究了黏弹性流体层流状态下流经突扩管时的局部阻力特性[8]。故可引用压力损失系数 ξ 来研究水煤浆流经弯管的局部阻力特性，即：

$$\xi = \Delta P_{bend} / \frac{1}{2}\rho v^2 \tag{5}$$

White 和 Mishra-Gupta 分别提出了用于计算较大曲率半径（$R_c/R > 12$）弯管的摩擦阻力损失之比与 De 关系的经验式[9~10]：

$$f_c/f_p = \left[1 - \left\{1 - \left(\frac{11.6}{De}\right)^{0.45}\right\}^{2.222}\right]^{-1} \tag{6}$$

$$f_c/f_p = 1 + 0.033(\log De)^{4.0} \tag{7}$$

其中：

$$De = Re\sqrt{R/R_c} \tag{8}$$

f_c 弯管段的摩擦阻力损失：

$$f_c = \frac{\Delta P_{bend}}{R_c \Delta\Theta} \frac{D}{2\rho v^2} \tag{9}$$

式中：$\Delta\Theta$—弯管的弯角。

f_p 弯管段前后稳定段的摩擦阻力损失：

$$f_p = 16/Re \tag{10}$$

2 实验以及结果分析

在东南大学洁净煤发电和燃烧技术教育部重点实验室的水煤浆输送试验装置上对不同曲率半径的 90°水平弯管（直径 D=50 mm）进行实验。实验采用神华煤，浓度为 56.7%，实验前已通过直管确定了水煤浆的流变模型，属于宾汉模型，本构方程为：τ = 20.588 16 + 0.162 73γ，由于试验管道中的流速较低，水煤浆的表观粘度较大，所以可以认为管内流动属于层流状态。

2.1 曲率半径对弯管的局部压力损失的影响

图 2 给出了不同曲率半径弯管的局部压力损失与雷诺数的关系。从图中可以看出，在较小雷诺数（Re<75）下，水煤浆流经弯管的局部压力损失较小且出现波动，其后随着雷诺数的增大，局部压力损失迅速地增加。

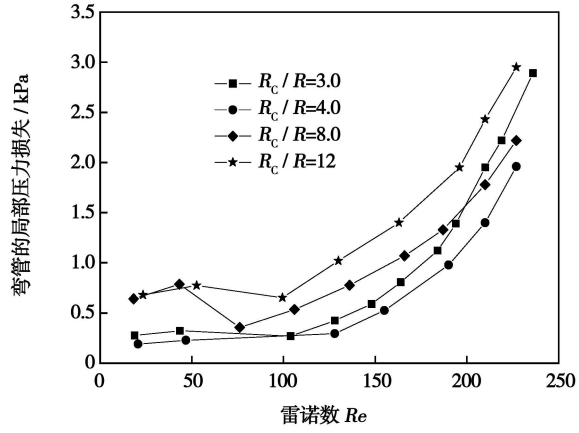

图 2 弯管的局部压力损失与雷诺数的关系

弯管的局部压力损失之所以波动，主要是因为水煤浆是一种具有触变性的非牛顿流体，在受到某一剪切之后内部结构遭到破坏，粘度降低，如果停止剪切，其内部结构又会缓慢恢复，粘度又会增大，从而导致再次启动时压力迅速增大。当水煤浆内部结构破坏与恢复达到平衡状态时，输送阻力也就稳定下来。

张中民认为水煤浆流经弯管的局部压力损失随着曲率半径 R_c 的增大而增加[11]。但在本次实验中，当雷诺数较大（Re> 100）时，对于小曲率半径弯管的局部压力损失并不符合上述趋势。在同一雷诺数下，R_c/R=4.0 的弯管局部压力损失为最小，R_c/R=12 的弯管局部压力损失最大，但是 R_c/R=3.0 的弯管局部压力损失却比 R_c/R=4.0 的弯管大。究其原因，主要是水煤浆流经弯管的局部压降由两个因素决定：不规则流动的影响和弯管轴线加长所带来的沿程阻力的影响。对于水煤浆这种高粘度流体，在弯管内更趋于规则流动，但是对于曲率半径较小的弯管，不规则流动因素的影响还是大于弯管轴线加长所造成的沿程阻力的影响。Marn 在研究灰水混合物流经小曲率半径弯管的局部阻力特性时，认为不规则流动所造成的阻力压降大于轴线加长造

成的沿程损失[12]。随着曲率半径的逐渐增大, 弯管轴线加长所造成的沿程阻力的影响将大于不规则流动的影响。

2.2　曲率半径对弯管的压力损失系数 ξ 的影响

由式(5)计算出水煤浆流经弯管的压力损失系数, 从而可以获得压力损失系数与雷诺数的关系。图 3 给出了不同曲率半径弯管的压力损失系数与雷诺数的关系。从图中可以看出, 弯管的压力损失系数随着雷诺数的增加而降低, 然后趋于稳定。但从对图中(图 3 的局部放大)可以发现, 随着雷诺数的增加, R_c/R 为 3.0 和 4.0 的弯管压力损失系数是逐渐增加的, 而 R_c/R 为 8.0 和 12 的弯管压力损失系数是先降后升, 且当 $Re<195$ 时, R_c/R 为 8.0 和 12 的弯管压力损失系数要高于 R_c/R 为 3.0 和 4.0 的弯管。Mam 认为当灰水混合物流经弯管时, 弯管的压力损失系数随着雷诺数($Re>500$)的增加而增加[12]。

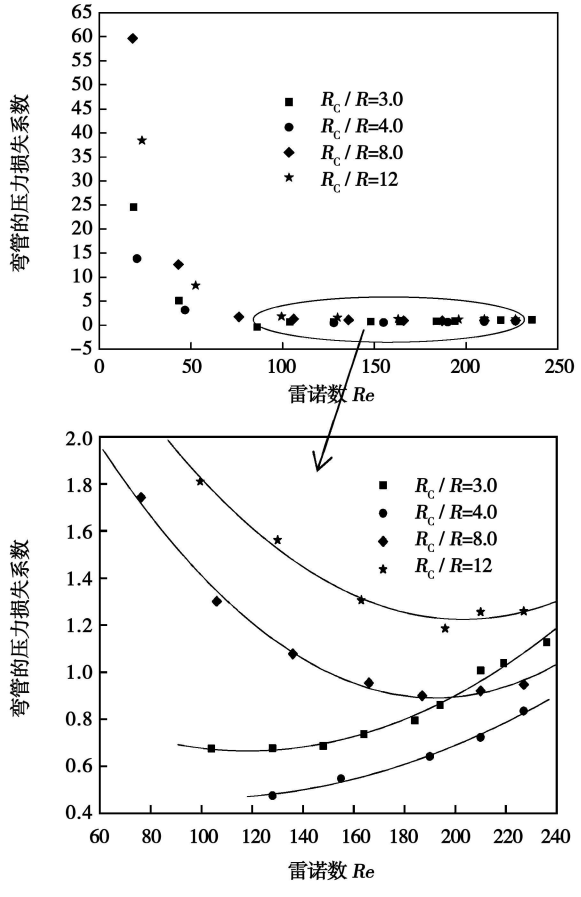

图 3　弯管的压力损失系数与雷诺数的关系

通过对图 3 的分析, 可以认为水煤浆流经弯管的压力损失系数随着雷诺数的增加先减少然后逐渐的增加, 且把压力损失系数由减少到增加的转折点所对应的雷诺数叫做转折雷诺数。从图中可以得到 R_c/R 为 8.0 和 12 的弯管转折雷诺数大约为 195, 而 R_c/R 为 3.0 和 4.0 的弯管转折雷诺数却比 R_c/R 为 8.0 和 12 的弯管小, 主要原因可能是随着弯管曲率半径的增加, 高粘度的水煤浆在弯管内不规则流动的程度减少, 所以必须在较大的雷诺数下才会出现压力损失系数的转变。

Mam 采用下式对灰水混合物流经弯管的压力损失系数和雷诺数的关系进行了拟合[7], 结果比较理想:

$$\xi = K_1 Re^{K_2} \tag{11}$$

式中: K_1、K_2—拟合待定系数。

运用式(11)对图 3 进行拟合时, 发现在较小雷诺数($Re<200$)情况下出现了较大的偏差。为了工程运用方便, 采用下式对图 3 进行拟合, 结果如表 1 所示。

$$\xi = K_1 + K_2 Re + K_3 Re^2 \tag{12}$$

表 1　压力损失系数与雷诺数拟合的结果

R_c/R	3.0	4.0	8.0	12
K_1	1.156 84	0.679 12	3.164 33	3.546 9
K_2	−0.008 3	−0.004 4	−0.023 7	−0.023
K_3	3.519 44E-5	2.210 28E-5	6.175 38E-5	5.636 1E-5

利用表 1 中的数据对相应弯管的压力损失系数进行计算时, 误差均小于 10%, 属于工程允许误差范围之内。

2.3　曲率半径对弯管摩擦阻力损失之比(f_c/f_p)的影响

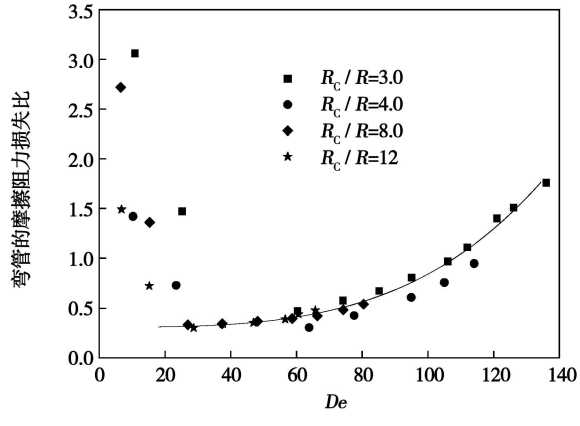

图 4　弯管的摩擦阻力损失比与 De 的关系

利用式(9)和式(10)可以分别求出水煤浆流经弯管的摩擦阻力损失 f_c 和 f_p, 从而获得弯管摩擦阻力损失之比与 De 的关系。图 4 给出了不同曲率半

径弯管的摩擦阻力损失之比与 De 的关系。由图所示,随着 De 的增加,弯管摩擦阻力损失之比先降低后逐渐增加。在 $20< De< 100$ 的情况下,R_c/R 为 3.0 的弯管摩擦阻力损失之比高于其它 3 种曲率半径弯管,R_c/R 为 4.0 的弯管摩擦阻力损失之比最小。Ternik 在研究非牛顿流体流经弯管的阻力特性时,得出了弯管摩擦阻力损失之比随着 De 的增加而增加的结论[13]。

Ternik、Marn 采用式(6)和式(7)拟合非牛顿流体流经弯管的摩擦阻力损失之比与 De 关系时,都出现了偏差[7, 13]。Marn 提出了一个与式(7)相似的式(13)来拟合[7],结果比较合理:

$$f_c/f_p=1+K_1(\log De)^{K_2} \tag{13}$$

但是采用式(7)和式(13)对图 4 进行拟合时,却出现了较大的误差。主要是因为灰水混合物是一种剪切变稠的非牛顿流体,而实验所用的水煤浆是一种剪切变稀的触变性非牛顿流体,并且本实验采用的是小曲率半径的弯管。Bandala-Rocha 认为非牛顿流体流经局部管件的阻力系数与资料所给出的阻力系数出现较大偏差[14],不但与局部管件的尺寸有关,而且与流体的流变特性有关。

采用式(14)对水煤浆流经小曲率半径弯管的摩擦阻力损失之比与 De 的关系进行拟合:

$$f_c/f_p=K_1+K_2(\log De)^{K_3} \tag{14}$$

式中:K_1、K_2、K_3—拟合待定系数。

考虑到刚开始流动的不稳定,只对图 4 中 $De>20$ 的实验数据进行拟合,结果为:

$K_1=0.300\ 87$、$K_2=0.000\ 021$、$K_3=14.300\ 86$

把拟合参数带入式(14)从而可以获得水煤浆流经小曲率半径弯管的摩擦阻力损失之比与 De 关系的经验式,但值得注意的是此经验式有一定的适用范围:$R_c/R\leqslant 12$,$20< De< 100$,超过这一范围就会出现较大的偏差。

3 结 论

通过对水煤浆流经不同小曲率半径的 90° 水平弯管的局部阻力特性分析,得到以下结论:

(1) 水煤浆具有明显的触变性,从而导致了流动开始时弯管局部压力损失的波动。

(2) 弯管的局部压力损失并不是随着曲率半径的增加而增加,而是由不规则流动的损失和弯管轴线加长所产生的沿程阻力决定的。

(3) 弯管的压力损失系数 ξ 随着雷诺数的增加先降低后增加。随着曲率半径的增加,临界雷诺数也会增大。

(4) 弯管的摩擦阻力损失之比随着 De 的增加先降低然后再增加。

(5) 水煤浆流经 R_c/R 为 4.0 的弯管的局部压力损失、压力损失系数以及摩擦阻力损失之比均最小。

参考文献:

[1] TURIAN R M, MA T W, GHSU F L, et al. Flow of concentrated non-newtonian slurries: 2. friction losses in bends, fittings, valves and venturi meters[J]. Int J Multiphase Flow, 1998, 24(2): 243—269.

[2] ETEMA GH S. Turbulent flow friction loss coefficients of fittings for purely viscous non-newtonian fluids[J]. Int Comm Heat Mass Transfer, 2004, 31(5): 763—771.

[3] TARUN KANTI BANDYOPADHYAY, SUDIP KUMAR DAS. Non-newtonian pseudoplastic liquid flow through small diameter piping components[J]. Petroleum Science and Engineering, 2007, 55: 156—166.

[4] NIGAM K D P, SHOBHA AGARWAL, SRIVASTAVA V K. Laminar convection of non-newtonian fluids in the thermal entrance region of coiled circular tubes [J]. Chemical Engineering Journal, 2001, 84: 223—237.

[5] SINGH R P, MISHRA P. Friction factor for newtonian and non-newtonian fluid flow in curved pipe[J]. J Chem Eng, 1980, 13: 275—280.

[6] MUKHTAR A, SINGH S N, SESHADRI V. Pressure drop in a long radius 90° horizontal bend for the flow of multisized heterogeneous slurries [J]. Int J Multiphase Flow, 1995, 21(2): 329—334.

[7] JURE MARN, PRIMOZ TERNIK. Laminar flow of a shear-thickening fluid in a 90° pipe bend[J]. Fluid Dynamics Research, 2006, 38: 295—312.

[8] OLIVEIRA P J. Asymmetric flows of viscoelastic fluids in symmetric planar expansion geometries[J]. J Non-Newtonian Fluid Mech, 2003, 114: 33—63.

[9] WHITE R G, FISHER M J, BERRY J F W. Test facilities techniques and instrumentation[J]. Journal of Sound and Vibration, 1973, 28(3): 619—622.

[10] MISHRA P, GUPTA S N. Momentum transfer in curved pipes, part 2: non-newtonian fluids[J]. Ind Eng Chem Process Des, 1979, 18: 137—142.

[11] 张中民. 水煤浆在水平 90 度弯管内流动阻力特性的研究[D]. 山东: 山东工业大学, 1989.

[12] MARN J, TERNIK P. Use of quadratic model for modeling of fly ash-water mixture[J]. Appl Rheol, 2003, 13: 286—296.

[13] TERNIK P, MARN J. Newtonian and non-newtonian fluid flow in a pipe bend //Proceedings of Kuhljevi dnevi 2003[C]. Zrečce: Slovensko društvo za mehaniko, 2003: 143—150.

[14] BANDALA ROCHA M R, MACEDO R C, RAMIREZ VELEZ RUIZ J F. Valuación de coeficientes de fricción en el transporte de fluidos no-newtonianos[J]. Inf Technol, 2005, 16: 73—80.

(编辑 韩 锋)

distribution model. If the integration format is properly chosen, the wide-band k distribution model can attain a calculation accuracy higher than that of the statistical narrow-band model, but comparable to that of the narrow-band k distribution model. For non-isothermal gases between ash wall plates, the calculation error of the wide-band k distribution model is about 10% when its calculation results are compared with those of the line-by-line calculation method, thus greatly enhancing the calculation accuracy and speed of gas radiative characteristics. **Key words**: carbon dioxide, wide-band k distribution model, radiative heat flux

选择性非催化脱硝不同还原剂的比较试验研究＝**A Contrast and Experimental Study of Various Reduction Agents for Selective Non-catalytic Denitration Process**[刊, 汉] / LI Ke-fu, WU Shao-hua, QIN Yu-kun (Combustion Engineering Research Institute, Harbin Institute of Technology, Harbin, China, Post Code: 150001), GAO Guan-shuai, LI Zhen-zhong (Technology Research Center of National Power Plant Combustion Engineering, Shenyang, China, Post Code: 110034) // Journal of Engineering for Thermal Energy & Power. — 2008, 23(4). —417 ~ 420

An experiment of selective non-catalytic reduction (SNCR) process was performed on a CRF (Combustion Research Facility) test rig. Carbamide, ammonia water, $(NH_4)_2CO_3$ and NH_4HCO_3 were used to reduce NO_X in flue gas and a reduction agent was sprayed into the CRF furnace through an atomization nozzle. The test results show that for the reduction agents used, with an increase of NH_3/NO molar ratio, the NO reduction efficiency will gradually increase. As for the reduction agents, such as carbamide, ammonia water and $(NH_4)_2CO_3$, NH_4HCO_3 etc., which have an ammonia/nitrogen molar ratio of 1 to 2.5, the denitration efficiencies will be 65%—89%, 62%—86% and 45%—84% respectively. As regards NH_4HCO_3 which has an ammonia/nitrogen molar ratio of 0.8 to 1.5, the denitration efficiency will be 46%—73%. The temperature windows of various reduction agents are different. The reaction temperature suitable for conducting the SNCR process is the highest for carbamide and the lowest for ammonia water. **Key words**: selective non-catalytic reduction (SNCR), NO_X, reduction agent, amido

安装倾角对热声发动机性能影响的试验研究＝**An Experimental Study of the Influence of Installation Inclination Angles on Thermoacoustic Engine Performance**[刊, 汉] / SHEN Chao, HE Ya-ling, LU Jie, et al (National Key Laboratory on Multiple-phase Flow in Power Engineering, College of Energy Source and Power Engineering, Xi'an Jiaotong University, Xi'an, China, Post Code: 710049) // Journal of Engineering for Thermal Energy & Power. — 2008, 23(4). —421 ~ 424

To fully utilize solar energy as a driving heat source, an experimental study was carried out of the thermodynamic performance of a standing-wave type thermoacoustic engine installed at various inclination angles. The test results show that the installation inclination angle of the thermoacoustic engine can exercise a remarkable influence on such parameters as the vibration-initiation temperature, vibration-fading temperature of the thermoacoustic system and temperature gradient in a plate stack during the initiation of vibration etc. When the nitrogen pressure in the system has reached 1.3 MPa, at the seven angles used during the experiment, the highest vibration initiation temperature is 484 ℃ and the lowest, 428 ℃. These characteristics can provide an experimental basis for choosing an appropriate angle to lower the vibration-initiation temperature of the system. When the system is in a stable oscillation state, any change of the installation inclination angle has a relatively small influence on such thermodynamic characteristics of the system as pressure ratio and pressure vibration amplitude. These characteristics create favorable conditions for driving at different angles thermoacoustic engines operating in a stable oscillation state by utilizing an auto-tracking solar energy collector. The test results can well provide an experimental basis for the design of solar-energy-driven thermoacoustic engines. **Key words**: thermoacoustic engine, natural convection, thermodynamic characteristics, solar energy

水煤浆流经小曲率半径弯管的阻力特性研究＝**A Study of Resistance Characteristics of Coal-water Slurry Passing Through a Tube Bend with a Small Curvature Radius**[刊, 汉] / LIU Meng, CHEN Liang-yong, DUAN Yu-feng (College of Energy Source and Environment, Southeast University, Nanjing, China, Post Code: 210096) // Journal of Engineering for Thermal Energy & Power. — 2008, 23(4). —425 ~ 428

On a self-made test stand, studied were the local resistance characteristics of water-coal slurry passing through a 90° horizontal tube bend with a small curvature radius along with an analysis of the influence of various curvature radii R_c on the

local pressure loss, pressure loss coefficient and friction resistance loss ratio of the bend. The results of the study show that with an increase of Reynolds Number Re, the local pressure loss of the bend will increase, but the pressure loss coefficient will first decrease and then increase. In view of the curvature radii being relatively small, the local pressure loss of the bend will be determined by the irregular flow loss and the path resistance produced by the lengthened axial line of the bend. The greater the curvature radius of the bend, the greater the critical Reynolds Number. The friction resistance loss ratio of the bend will first go down and then up with an increase of Dean Number. When the R_c/R of the bend equals 4, its local pressure loss, pressure loss coefficient and friction resistance loss ratio will all attain a minimum value. **Key words**: coal-water slurry, curvature radius, pressure loss coefficient, critical Reynolds Number

生物质再燃脱硝特性研究=**Research on Biomass Reburning Denitration Characteristics**[刊, 汉] / GAO Pan, LU Chun-mei (College of Energy Source and Power Engineering, Shandong University, Jinan, China, Post Code: 250061), RUAN Lei (Construction Preparation Division, Dingzi Mountain Heat Source Sub-factory, Jinan City Southern Suburb Thermal Power Plant, Jinan, China, Post Code: 250002), LIU Zhi-chao (Thermal Energy Research Institute, Shandong Electric Power Academy, Jinan, China, Post Code: 250002)// Journal of Engineering for Thermal Energy & Power. —2008, 23(4). —429 ~433

A multi-purpose denitration test rig was utilized to study the reburning denitration characteristics of aspen wood sawdust, peanut shell, rice husk and cornstalk under the condition of typical influencing factors on reburning denitration. The test results show that when the furnace temperature is between 700 ~900 ℃, increasing the reburning temperature will result in a rapid increase of the precipitation speed of volatile matter in biomass followed by a quick enhancement of the denitration rate. At a temperature higher than 900 ℃, the precipitation of the volatile matter attains a saturation state and a relatively high furnace temperature tends to make the biomass to be heated, which leads to coke formation, enhancing the positive pressure of the furnace and causing the denitration rate to drop somewhat. The stoichiometric ratio (SR) has a relatively similar influencing effect for the reburning denitration of the materials under experiment. Four kinds of biomass all attain their highest denitration efficiency when SR=0.8. Under the same conditions, the smaller the biomass particle diameter, the greater the initial NO concentration and the better the reburning denitration effectiveness. A relatively big reburning fuel ratio (RFR) can compensate to a certain extent the difference in the denitration rate brought about by the reburning material particle diameter and initial NO concentration. To extend the residence duration t in the renurning zone is favorable to enhancing the denitration rate. However, when t > 0.81 second, its influence on the denitration rate will not be significant. **Key words**: biomass, reburning, denitration rate, experiment

季节条件对于地源热泵系统运行的影响=**Effect of Seasonal Conditions on the Operation of a Geothermal Pump System**[刊, 汉] / LIU Xiang-yun, CHEN Ying, YANG Min (College of Material and Energy Source, Guangdong Polytehnical University, Guangzhou, China, Post Code: 510006)// Journal of Engineering for Thermal Energy & Power. —2008, 23(4). —434 ~437

With the continuous consumption of conventional energy sources, the demand of human beings for regenerative energy sources will grow with each passing day. As a kind of advanced, highly effective, energy-saving and environment-protection technology, geothermal pumps have attracted the attention of numerous researchers. The geothermal pumps can make use of the constant temperature under buildings to take the heat/cooling energy under the ground, achieving a good quality of zero pollution. Through experiments, the effect of different conditions in winter and summer on the operation of a geothermal pump system has been compared. The authors have come to the following conclusion: if the heat or cooling energy under the ground is taken purely and simply, a remarkable change will occur to the underground temperature around the geothermal pumps after three months, causing the system impossible to continue its normal operation. Only when a mode of alternatively taking heat and cooling energy under the ground is adopted for the geothermal pump systems, will the underground soil retain its ability to serve as a heat source. **Key words**: climatic condition, geothermal pump, soil temperature, mode